Supporting Information

Engineering of platinum-oxygen vacancy interfacial sites in confined catalysts for enhanced hydrogenation selectivity

Mi Xiong,[a,b] Guofu Wang,[a] Shichao Zhao,[a] Zhengxing Lv,[c] Shuangfeng Xing,[a,b] Jianyuan Zhang,[a,b] Bianqin Zhang,[a,b] Yong Qin[a,b] and Zhe Gao*[a]

[a] State Key Laboratory of Coal Conversion, Institute of Coal Chemistry, Chinese Academy of Sciences, Taiyuan 030001, China.

[b] Center of Materials Science and Optoelectronics Engineering, University of Chinese Academy of Sciences, Beijing 100049, China.

[c] Shanghai Synchrotron Radiation Facility, Shanghai Institute of Applied Physics, Chinese Academy of Sciences, Shanghai 201204, China.

Experimental section

1.1 Synthesis of catalysts.

Synthesis of CNCs and the ALD process. The carbon nanocoils (CNCs) were synthesized by chemical vapor deposition using acetylene as a carbon source and copper nanoparticles as catalysts at 250 °C followed by a heat treatment at 900 °C in an Ar atmosphere for 2 h. Raw CNCs were refluxed in HNO_3 (15 wt %) for 4 h at 100 °C in an oil bath to remove the copper catalysts, then filtered and washed with deionized water and ethanol until there was no further change in pH (around pH = 7).

The atomic layer deposition (ALD) process was carried out in a hot-wall closed chamber-type ALD reactor. Prior to ALD, 15 mg CNCs were dispersed onto a quartz wafer (5 cm×10 cm) with ethanol. After the samples were dried at ambient temperature, they were transferred to the ALD chamber. Pt nanoparticles were deposited at 250 °C with trimethyl (methylcyclopentadienyl) platinum ($MeCpPtMe_3$) and ozone (O_3) as precursors. $MeCpPtMe_3$ was kept at 65 °C. The pulse, exposure, and purge times for the $MeCpPtMe_3$ were 0.5, 12, and 25 s, respectively, and for the O_3, 0.1, 12, and 25 s, respectively. The TiO_2 film was deposited at 125 °C with titanium tetraisopropoxide (TTIP) and deionized H_2O as precursors. The pulse, exposure, and purge times for the TTIP were 1, 8, and 25 s, respectively, and for the H_2O, 0.1, 8, and 25 s, respectively.

Synthesis of TiO_2/Pt. CNCs were firstly decorated with Pt nanoparticles (20 cycles) by Pt ALD and then coated with a TiO_2 layer (300 cycles) by TiO_2 ALD, producing TiO_2/Pt/CNCs. The TiO_2/Pt/CNCs was calcinated at 500 °C for 2 h to remove the CNC templates, obtaining a TiO_2/Pt catalyst, in which Pt nanoparticles were confined in TiO_2 nanotubes.

Synthesis of TiO_2/Pt-T-Ar. The TiO_2/Pt/CNCs prepared by the above method was firstly heated under argon atmosphere at different temperatures (T=500 °C, 600 °C, 700 °C, and 800 °C) for 2 h. After the thermal treatment, the obtained sample was calcinated at 500 °C for 2 h to remove the CNC templates, obtaining a TiO_2/Pt-T-Ar catalyst.

Synthesis of Pt/TiO_2 and Pt/TiO_2-700-Ar. CNCs were firstly coated with a TiO_2 layer (300 cycles) by TiO_2 ALD and then decorated with Pt nanoparticles (20 cycles) by Pt ALD, producing Pt/TiO_2/CNCs. Next, the Pt/TiO_2/CNCs was calcined at 500 °C for 2 h, obtaining a Pt/TiO_2 catalyst, in which Pt nanoparticles were supported on the outer surfaces of TiO_2 nanotubes. When the Pt/TiO_2/CNCs was firstly heated under argon atmosphere at 700 °C for 2 h and then calcined at 500 °C for 2 h, the Pt/TiO_2-700-Ar was obtained.

1.2 Catalyst characterizations.

Transmission electron microscopy (TEM) images, high-angle annular dark field scanning transmission electron microscopy (HAADF-STEM) images, and energy-dispersive X-ray spectroscopy (EDS) mapping profiles were acquired with a JEM-2100F field-emission transmission electron microscope operated at 200 kV. X-ray diffraction (XRD) patterns were collected on a Bruker D8 Advance X-ray diffractometer using a Cu Kα source (λ = 1.540 Å) in the 2θ range from 10° to 90°. The

N_2 sorption measurements were performed using Micromeritics Tristar II (3020) at 77 K. The contents of Pt metal in the catalysts were determined by inductively coupled plasma atomic emission spectrometry (ICP-AES, Thermo iCAP 6300).

X-ray photoelectron spectra (XPS) were recorded on an AXIS ULTRA DLD spectrometer (Shimadzu/Kratos) to characterize the surface composition with the Al Kα line as the excitation source. The C 1s peak at 284.8 eV was used as a reference for calibration. XPS spectra of the catalysts without exposure to air were obtained based on the assistance of a pretreatment chamber. The carbon-assisted thermal treatment under argon atmosphere for TiO_2/Pt/CNCs was performed in tubular furnace. The calcination under flowing air (500 °C, 2 h) for TiO_2/Pt/CNCs and TiO_2/Pt/CNCs-700-Ar was performed in the pretreatment chamber connected by an in-vacuum sample transfer system to the surface analysis chamber. Therefore, the samples treated in the pretreatment chamber can be transferred to the analysis chamber without exposure to air.

Electron paramagnetic resonance (EPR) spectra were recorded using a Brucker EMX spectrometer (EMXplus-10/12) operating at 100 kHz field modulation. The signal intensities of EPR spectra for different catalysts were quantified using a double integration method of the peaks based on the area under the curve.

The X-ray absorption near-edge structure (XANES) and extended X-ray absorption fine structure (EXAFS) spectra of the Ti K-edge were measured on the BL11B beamline of the Shanghai Synchrotron Radiation Facility (SSRF), Shanghai Advanced Research Institute, Chinese Academy of Sciences. A Si (111) double-crystal monochromator was used to reduce the harmonic component of the monochrome beam. Anatase TiO_2 was used as the reference sample and measured in the transmission mode, and all the catalysts were measured in the transmission mode. IFEFFIT software was used to calibrate the energy scale, to correct the background signal and to normalize the intensity. The theoretical paths for Ti–O and Ti–Ti species used for fitting two coordination shells of the experimental data were generated using the FEFF7 program. The coordination number, bond distance, Debye–Waller factor, and inner potential correction were used as variable parameters for the fitting procedures.

Diffuse reflectance infrared Fourier transform spectroscopy (DRIFTS) spectra were recorded using a Bruker Tensor II spectrometer with a resolution of 2 cm^{-1}. The IR spectrum of TiO_2/Pt-700-Ar without exposure to air was obtained based on in-situ calcination in a DRIFTS cell. TiO_2/Pt/CNCs was firstly heated under argon atmosphere in tubular furnace. Then the obtained TiO_2/Pt/CNCs-700-Ar was placed into the DRIFTS cell and calcinated under oxygen flow for the removal of CNCs. After calcination, the spectrum was recorded in argon atmosphere. Temperature-programmed desorption of *p*-nitrobenzyl chloride (*p*-NBC) over different catalysts was also performed in a DRIFTS cell. As a typical run, the sample was placed in the DRIFTS cell and treated under Ar flow at 200 °C for 1 h. After that, 20 μL methanol solution of *p*-NBC was injected into the cell by a homemade window at 55 °C. The heating rate was 10 °C/min. The spectra at different temperatures (55, 65, 75, 85, 100, 150, and 200 °C) were collected when *p*-NBC was not desorbed from the catalyst surfaces.

1.3 Catalytic hydrogenation tests.

p-NBC hydrogenation reactions over the catalysts were carried out in a 50 mL stainless-steel autoclave reactor. The reaction was carried out at 55 °C and 1 MPa H_2 with 10 mg of catalyst, 0.5 mmol of *p*-NBC and 20 mL of anhydrous methanol. After the reaction, the reactor was cooled and then slowly depressurized. Finally, the reaction mixture was separated by centrifugation in order to remove the solid catalysts. The reaction products were analyzed and quantified by gas chromatographic mass spectrometry (GC-MS, Agilent Technologies 7890A-5975C). The reaction conversion and selectivity were determined by the product analysis.

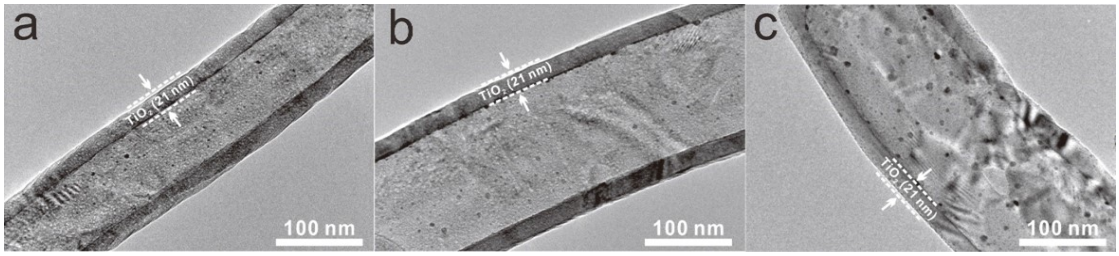

Figure S1. TEM images of (a) TiO_2/Pt-500-Ar, (b) TiO_2/Pt-600-Ar, and (c) TiO_2/Pt-800-Ar.

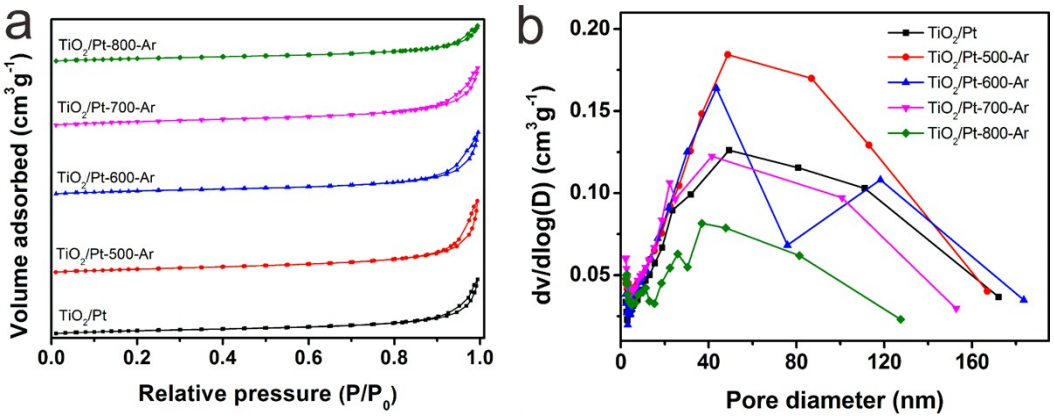

Figure S2. (a) The N_2 adsorption-desorption isotherms and (b) the corresponding pore size distributions for TiO_2/Pt and TiO_2/Pt-T-Ar. Brunauer-Emmett-Teller (BET) surface areas, pore volumes, and average pore diameters of the catalysts are listed in Table S1.

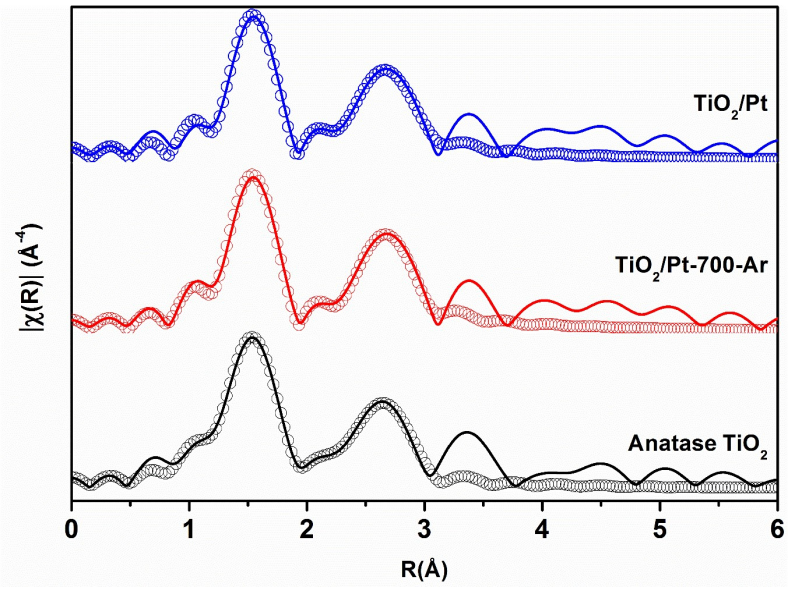

Figure S3. The EXAFS spectra and their k^3-weighted fitting spectra of anatase TiO_2, TiO_2/Pt, and TiO_2/Pt-700-Ar. Lines indicate experimental data and open circles indicate fitted results.

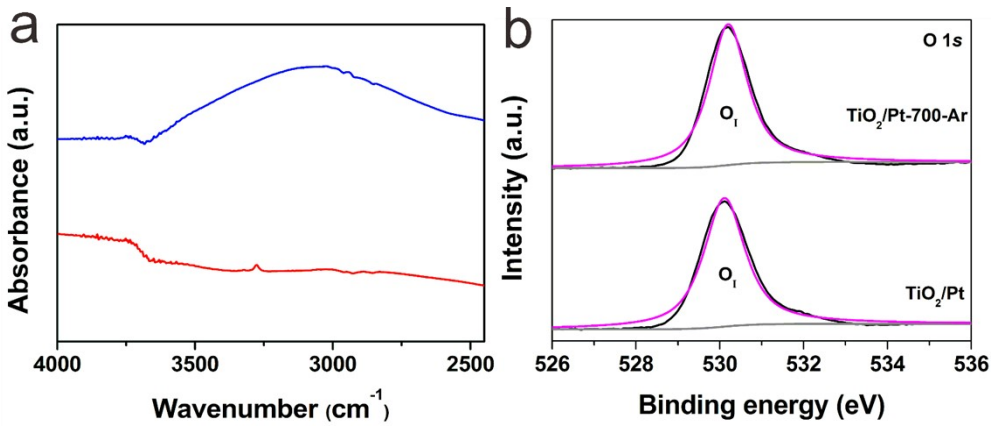

Figure S4. (a) The IR spectra of TiO_2/Pt-700-Ar with exposure (blue line) and without exposure (red line) to air. (b) The XPS O 1s spectra of TiO_2/Pt and TiO_2/Pt-700-Ar without exposure to air. The spectrum (Figure S4a, blue line) shows a broad adsorption band at 3000~3700 cm^{-1} corresponding to the surface-adsorbed water and the hydroxyl groups. For the TiO_2/Pt-700-Ar without exposure to air, no OH stretching features in the range 3700–3300 cm^{-1} is observed (Figure S4a, red line), meaning few surface hydroxyls. In Figure S4b, only a peak at ~530.0 eV is observed and no shoulder peak is observed at 531.8 eV. This may be because the catalysts were not exposed to air and there are no hydroxyl groups formed by dissociative adsorption of H_2O on oxygen vacancies of TiO_2 surfaces.

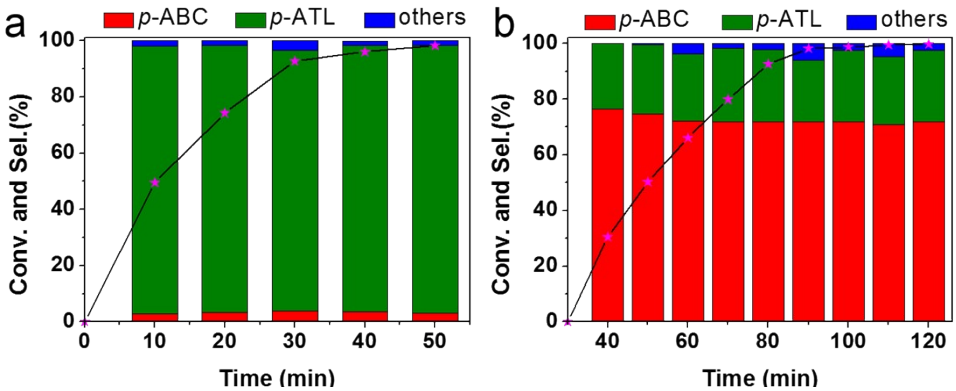

Figure S5. The evolution of *p*-nitrobenzyl chloride conversion and product selectivities with reaction time over (a) TiO_2/Pt and (b) TiO_2/Pt-700-Ar. The *p*-ABC and *p*-ATL represent *p*-aminobenzyl chloride and *p*-aminotoluene, respectively. Others include *p*-nitrotoluene, *p*-nitrosotoluene, and *p*-hydroxyamine toluene.

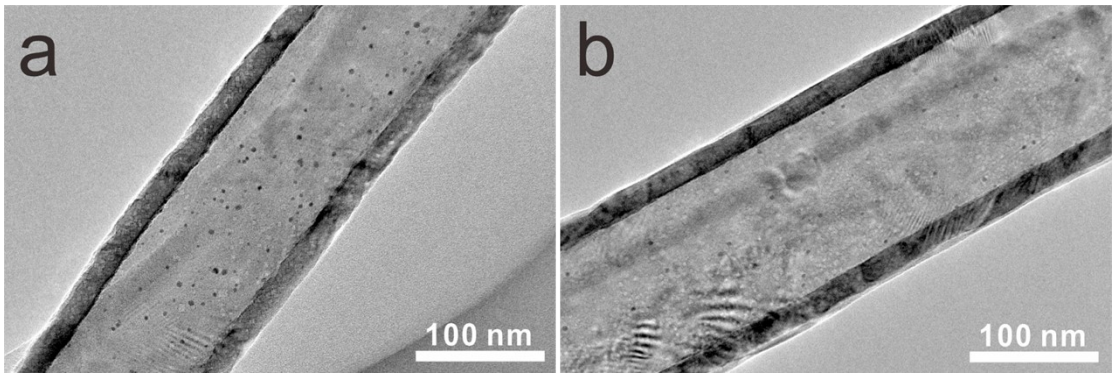

Figure S6. TEM images of (a) TiO_2/15Pt-700-Ar and (b) TiO_2/10Pt-700-Ar.

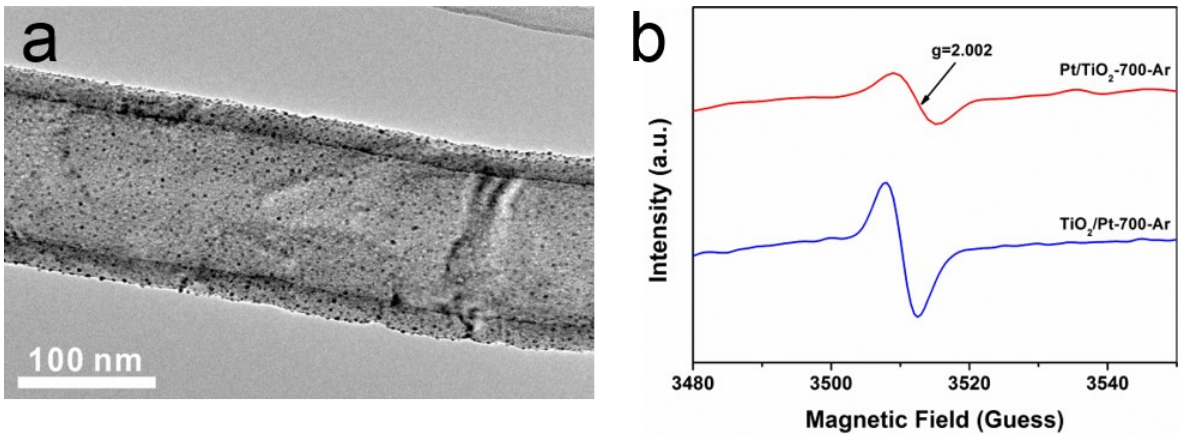

Figure S7. (a) TEM images of Pt/TiO_2-700-Ar. (b) The EPR spectra of Pt/TiO_2-700-Ar and TiO_2/Pt-700-Ar.

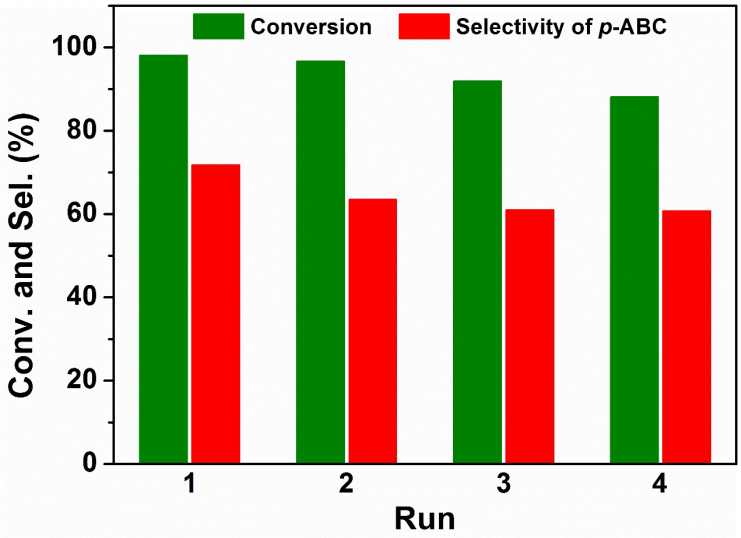

Figure S8. The recycling stability of TiO_2/Pt-700-Ar in the hydrogenation of *p*-NBC.

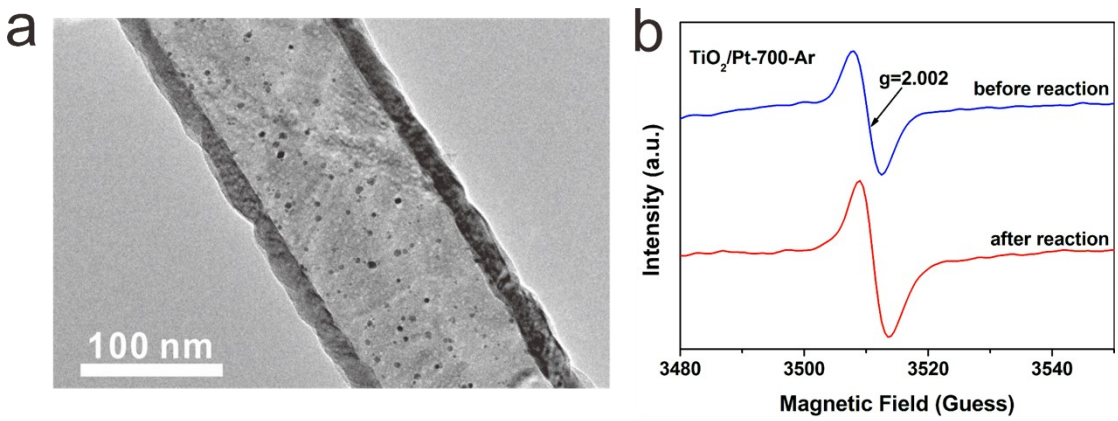

Figure S9. (a) TEM image of TiO_2/Pt-700-Ar after four consecutive runs. (b) EPR spectra of TiO_2/Pt-700-Ar before and after reaction.

Table S1. The specific surface areas and pore structure parameters of TiO_2/Pt and TiO_2/Pt-T-Ar.

Catalysts	S_{BET} (m^2 g^{-1})	V_{total} (cm^3 g^{-1})	D (nm)
TiO_2/Pt	40.5	0.14	49.3
TiO_2/Pt-500-Ar	46.2	0.18	48.8
TiO_2/Pt-600-Ar	45.0	0.16	43.6
TiO_2/Pt-700-Ar	48.0	0.15	41.5
TiO_2/Pt-800-Ar	36.0	0.09	37.0

Table S2. Loading amounts of Pt for different catalysts.

Sample	Pt contents (wt.%)
TiO_2/Pt	0.46
TiO_2/Pt-700-Ar	0.49
TiO_2/15Pt-700-Ar	0.42
TiO_2/10Pt-700-Ar	0.32
Pt/TiO_2	1.56
Pt/TiO_2-700-Ar	1.32

Table S3. EXAFS data fitting results of anatase TiO_2, TiO_2/Pt, and TiO_2/Pt-700-Ar.

Sample	Shell	CN	R (Å)	$\Delta\sigma^2\times10^3$ (Å^2)	R-factor(%)
TiO_2	Ti-O	6	1.96	5.7±0.2	0.6
	Ti-Ti	4	3.05	5.5±0.3	
TiO_2/Pt	Ti-O	5.9	1.95	1.8±0.4	0.3
	Ti-Ti	3.0	3.05	1.9±0.5	
TiO_2/Pt-700-Ar	Ti-O	5.0	1.95	3.0±0.6	0.7
	Ti-Ti	3.5	3.05	1.4±0.7	

Table S4. Area under the curve (AUC) of EPR spectra for different catalysts.

Catalysts	AUC
TiO_2/Pt	0
TiO_2/Pt-500-Ar	0
TiO_2/Pt-600-Ar	0
TiO_2/Pt-700-Ar	14.2
TiO_2/Pt-700-Ar (after reaction)	17.9
TiO_2/Pt-800-Ar	95.6
Pt/TiO_2-700-Ar	4.1

Table S5. The position (P_{peak}), area (A_{peak}), and O_{II}/O_I area ratio of XPS O 1s peak for TiO_2/Pt and TiO_2/Pt-700-Ar.

Catalysts	O_I		O_{II}		Area ratio
	P_{peak}	A_{peak}	P_{peak}	A_{peak}	(O_{II}/O_I)
TiO_2/Pt	530.0	112702.6	531.8	3811.9	0.03
TiO_2/Pt-700-Ar	530.1	117108.7	531.8	12403.6	0.11

Table S6. Catalytic performances of the TiO_2/Pt-700-Ar catalysts with different Pt ALD cycles for *p*-nitrobenzyl chloride hydrogenation.

Catalysts	Time (min)	Conv. (%)	Sel. (%)[a]		
			p-ABC	*p*-ATL	others
TiO_2/15Pt-700-Ar	110	99.5	73.3	17.8	8.9
TiO_2/10Pt-700-Ar	140	95.8	75.7	11.7	12.6

[a]The *p*-ABC and *p*-ATL represent *p*-aminobenzyl chloride and *p*-aminotoluene, respectively. Others include *p*-nitrotoluene, *p*-nitrosotoluene, and *p*-hydroxyamine toluene.

Table S7. Catalytic performances of unconfined Pt/TiO_2 and Pt/TiO_2-700-Ar and confined TiO_2/Pt-500-H_2 for *p*-nitrobenzyl chloride hydrogenation.

Catalysts	Time (min)	Conv. (%)	Sel. (%)[a]		
			p-ABC	*p*-ATL	others
Pt/TiO_2	30	92.4	2.0	93.8	4.2
Pt/TiO_2-700-Ar	90	94.5	4.4	93.6	2
TiO_2/Pt-500-H_2[b]	90	93.8	56.2	32.9	10.9

[a]The *p*-ABC and *p*-ATL represent *p*-aminobenzyl chloride and *p*-aminotoluene, respectively. Others include *p*-nitrotoluene, *p*-nitrosotoluene, and *p*-hydroxyamine toluene.

[b]Reducing TiO_2/Pt at 500 ^oC for 1 h.

Notes: Compared to hydrogen reduction to create oxygen vacancies by gas-solid reaction (H_2 and TiO_2), the carbon-assisted thermal treatment creates oxygen vacancies by solid-solid reaction (carbon and TiO_2). The gas-solid reaction forms oxygen vacancies on the whole TiO_2, while the solid-solid reaction can selectively generate oxygen vacancies in the interfacial region between carbon and TiO_2. This provides more alternative means for regulation of interfacial sites, which will contribute to further interfacial site optimization and performance improvement. Moreover, from the perspective of safety, the carbon-assisted thermal treatment also shows the superiority.

Compared to hydrogen reduction, additional calcination in air for the carbon-assisted thermal treatment is required to remove the carbon templates after oxygen vacancies are generated.